Paraxial and ray approximations of acoustic vortex beams

Chirag A. Gokani   Michael R. Haberman   Mark F. Hamilton

Applied Research Laboratories & Walker Department of Mechanical Engineering
University of Texas at Austin

CLND Group Meeting, September 25th, 2024

The University of Texas at Austin
Walker Department
of Mechanical Engineering
Cockrell School of Engineering

Outline

Outline

Lindsay's wheel of acoustics

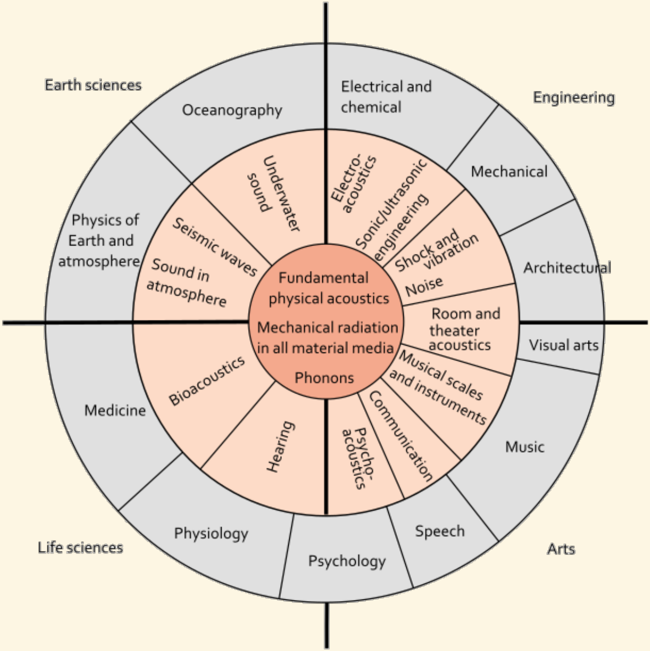

What is sound?

$$\frac{\partial \rho}{\partial t} + \boldsymbol{\nabla} \cdot (\rho \mathbf{u}) = 0$$

$$\rho \frac{\partial \mathbf{u}}{\partial t} + (\rho \mathbf{u} \cdot \boldsymbol{\nabla}) \mathbf{u} + \boldsymbol{\nabla} P = (\lambda + 2\mu) \boldsymbol{\nabla} (\boldsymbol{\nabla} \cdot \mathbf{u}) - \mu \boldsymbol{\nabla} \times \boldsymbol{\nabla} \times \mathbf{u}$$

$$\rho C_v \frac{DT}{Dt} + P \boldsymbol{\nabla} \cdot \mathbf{u} = \Phi^{(\mathrm{visc})} + \kappa \nabla^2 T$$

$$P = P(\rho, s)$$

- A wave equation that accounts for diffraction, losses, and nonlinearity is

$$\Box^2 p + \frac{\delta}{c_0^4} \frac{\partial^3 p}{\partial t^3} + \frac{\beta}{\rho_0 c_0^4} \frac{\partial^2 p^2}{\partial t^2} = 0 \,. \qquad \text{(Westervelt, 1963)}$$

- A simpler description of sound is the linear pressure wave equation:

$$\nabla^2 p - \frac{1}{c_0^2} \frac{\partial^2 p}{\partial t^2} = 0 \,. \tag{1}$$

What is an acoustic vortex beam?

Characterized by...

- helical wavefronts
- orbital number $\ell =$ number of equiphase wavefronts in $\perp$ plane
- zero acoustic pressure on axis

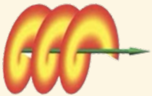

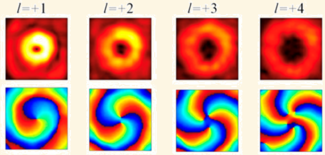

C. Shi et al. 2017,
P. Natl. Acad. Sci. U.S.A.

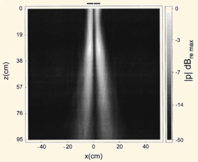

B. T. Hefner and P. L. Marston
1999, *J. Acoust. Soc. Am.*

What is an acoustic vortex beam?

Generated by...

- phase plates
- transducer arrays
- metasurfaces

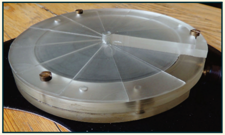

M. E. Terzi et al. 2017, *Moscow University Physics Bulletin*

A. Marzo, M. Caleap, and B. W. Drinkwater 2018, *Phys. Rev. Lett.*

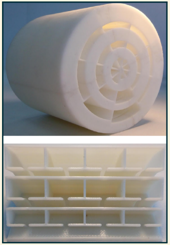

X. Jiang et al. 2016, *Phys. Rev. Lett.*

What is an acoustic vortex beam?

Used for...

- particle manipulation
- underwater communications
- therapeutic biomedical ultrasound
- sound diffusion[1]

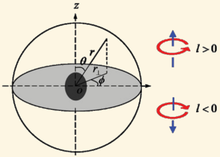

Zhang and Marston 2011, *Phys. Rev. E*

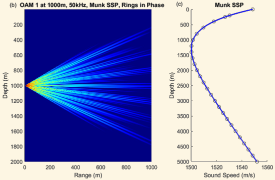

M. E. Kelly and C. Shi 2023, *JASA Express Lett.*

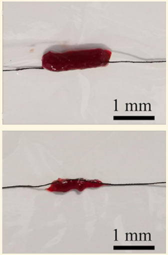

S. Guo et al. 2022, *Ultrasound Med. Biol.*

[1] N. Jiménez, J. -P. Groby, and V. Romero-García 2021, *Sci. Rep.*

Outline

Paraxial equation and its integral solution

- For $p = qe^{i(kz-\omega t)}$ and $|\partial^2 q/\partial z^2| \ll 2k|\partial q/\partial z|$, Eq. (1) becomes

$$i2k\frac{\partial q}{\partial z} + \nabla_\perp^2 q = 0\,. \tag{2}$$

- $\nabla_\perp^2$ is the Laplacian in the plane perpendicular to the z axis.
- Equation (2) is solved by the Fresnel diffraction integral:

$$q(r,\theta,z) = -\frac{ik}{2\pi z}\int_0^{2\pi}\int_0^{\infty} q(r_0,\theta_0,0)\, e^{i(k/2z)[r^2+r_0^2-2rr_0\cos(\theta_0-\theta)]}\, r_0\, dr_0\, d\theta_0\,,$$

where $q(r_0,\theta_0,0)$ is the prescribed pressure field in the plane $z=0$.

- A Gaussian focused vortex source condition is considered:

$$q(r,\theta,0) = p_0\, e^{-r^2/a^2}\, e^{-ikr^2/2d}\, e^{i\ell\theta}\,. \tag{3}$$

Closed-form solution for Gaussian vortex source

- The solution of Eq. (2) for Eq. (3) is

$$q(r,\theta,z) = \sqrt{8\pi}\,\frac{p_0 z}{kr^2}\chi^{3/2}e^{-\chi}\left[I_{(\ell-1)/2}(\chi) - I_{(\ell+1)/2}(\chi)\right] \times\ e^{i[\ell\theta-(\ell+1)\pi/2+kr^2/2z]}\,, \tag{4}$$

$$\chi(r,z) = \frac{\frac{1}{8}(kar/z)^2}{1-i(ka^2/2z)(1-z/d)}\,. \tag{5}$$

- For $\ell = 0$, a focused Gaussian beam[2] is recovered, where $G = ka^2/2d$:

$$q(r,z) = \frac{p_0}{1-(1-iG^{-1})z/d}\exp\left[-\frac{(1+iG)r^2/a^2}{1-(1-iG^{-1})z/d}\right], \quad \ell = 0\,. \tag{6}$$

- For an unfocused source $(d = \infty)$ with no vorticity $(\ell = 0)$, Eq. (4) reduces to

$$q(r,z) = \frac{p_0}{1+iz/z_R}\exp\left(-\frac{r^2/a^2}{1+iz/z_R}\right), \quad z_R = ka^2/2\,. \tag{7}$$

[2] "Nonlinear Acoustics," M. F. Hamilton and D. T. Blackstock, 2008. Eqs. (8.19) and (8.37).

An equivalent solution: Laguerre-Gaussian modes

- The eigenfunctions of Eq. (2) are

$$\mathrm{LG}_{nm}(r,\theta,z) = \frac{N_n^m}{w(z)}\left(\frac{\sqrt{2}r}{w(z)}\right)^{|m|} L_n^{|m|}\left(\frac{2r^2}{w^2(z)}\right)\exp\left(-\frac{r^2}{w^2(z)}\right) \times \exp\left\{i\left[m\theta + \frac{kr^2}{2R(z)} - (2n+|m|+1)\phi(z)\right]\right\}, \quad (8)$$

  where L_n^m are the Laguerre polynomials.
- The following quantities are defined with respect to $z_w = kw_0^2/2$:

$$w(z) = w_0\sqrt{1+(z/z_w)^2}\,, \quad R(z) = z[1+(z_w/z)^2]\,, \quad \phi(z) = \arctan(z/z_w)\,,$$

- $N_n^m = \{2n!/[\pi(n+|m|)!]\}^{1/2}$ is a normalization factor such that

$$\int_0^{2\pi}\int_0^{\infty} \mathrm{LG}_{nm}(r,\theta,z)\mathrm{LG}^*_{n'm'}(r,\theta,z)\, r\, dr d\theta = \delta_{nn'}\delta_{mm'}\,. \quad (9)$$

An equivalent solution: Laguerre-Gaussian modes

- The general solution of Eq. (2) is

$$q(r,\theta,z) = \sum_{n,m} A_n^m \mathrm{LG}_{nm}(r,\theta,z) \tag{10}$$

- Matching the boundary condition and invoking orthogonality yields

$$q(r,\theta,z) = p_0\, e^{i\theta} \frac{r/a}{|\zeta(z)|^2} \exp\left(-\frac{r^2/a^2}{\zeta(z)}\right) \times \sqrt{\pi/2} \sum_{n=0}^{\infty} \frac{(2n)!\; e^{-i(2n+2)\phi_R(z)}}{4^n(n+1)(n!)^2} L_n^1\left(\frac{2r^2/a^2}{|\zeta(z)|^2}\right), \quad \ell = 1, \tag{11a}$$

$$q(r,\theta,z) = p_0\, e^{i2\theta} \frac{r^2/a^2}{|\zeta(z)|^3} \exp\left(-\frac{r^2/a^2}{\zeta(z)}\right) \times 2 \sum_{n=0}^{\infty} \frac{e^{-i(2n+3)\phi_R(z)}}{(n+1)(n+2)} L_n^2\left(\frac{2r^2/a^2}{|\zeta(z)|^2}\right), \quad \ell = 2, \tag{11b}$$

where $\zeta(z) = 1 + iz/z_R$, $\phi_R(z) = \arctan(z/z_R)$, and $z_R = ka^2/2$.

- $\sim$10 and 20 terms of Eqs. (11a) and (11b) are required for convergence.

Vortex ring radius

- Focused beams used for particle manipulation
- Magnitudes of vortex beam fields are axisymmetric
- In geometric focal plane $z = d$, field forms toroidal ring
- Analytical solution (4) can be used to find the radius of this ring

D. Baresch, J. -L. Thomas, and R. Marchiano 2016, *Phys. Rev. Lett.*

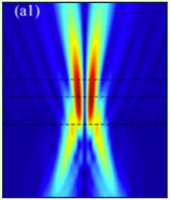

C. Zhou et al. 2020, *J. Appl. Phys.*

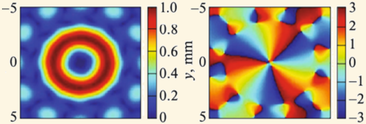

M. E. Terzi et al. 2017, *Moscow University Physics Bulletin*

Vortex ring radius

- The vortex ring radius is found by setting $\partial|q|/\partial r = 0$.
- For real χ, $\partial|q|/\partial r = 0$ equals

$$\frac{d}{d\chi}\left\{\chi^{1/2}e^{-\chi}\left[I_{(\ell-1)/2}(\chi) - I_{(\ell+1)/2}(\chi)\right]\right\} = 0\,. \tag{12}$$

- Evaluating Eq. (12) and finding the roots numerically yields the ring radii,

$$\begin{aligned} r_\ell &= \eta_\ell d/ka\,, \quad z = d\,, && (13)\\ &= \eta_\ell z/ka\,, \quad d = \infty\,, \quad z \gg z_R\,, && (14)\end{aligned}$$

where $\eta_\ell = 0.9405\ell + 0.7518$.

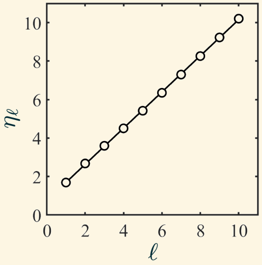

Vortex radiation from unfocused circular piston

- Gaussian amplitude distributions accurately describe laser sources.[3]
- But acoustic sources are more commonly described by

$$q(r,\theta,0) = p_0 \,\mathrm{circ}(r/a)\, e^{i\ell\theta}\,, \tag{15}$$

  where $\mathrm{circ}(x) = 1$ for $0 \leq x \leq 1$ and 0 for $x > 1$.
- Insertion in the Fresnel diffraction integral leads to

$$q = -ikp_0 \frac{e^{i(ka^2/2z)r^2/a^2}}{z}\, e^{i\ell(\theta-\pi/2)} \int_0^a e^{i(ka^2/2z)r_0^2/a^2} J_\ell(krr_0/z)\, r_0\, dr_0\,. \tag{16}$$

- Equation (16) reduces to

$$q = -ikp_0 \frac{1}{z} e^{i\ell(\theta-\pi/2)} \int_0^a J_\ell(krr_0/z)\, r_0\, dr_0 \tag{17}$$

  for $z \gg z_R$, where $z_R = ka^2/2$ is the Rayleigh distance.

[3] V. V. Kotlyar, A. A. Kovalev, and A. P. Porfirev 2018.

Vortex radiation from unfocused circular piston

- Taking the integral leads to an analytical solution:

$$q_\ell(r,\theta,z) = -ip_0\,\frac{z}{kr^2}\,e^{i\ell(\theta-\pi/2)}\,F_\ell(kar/z)\,,\quad z \gg z_R\,, \tag{18}$$

where[4]

$$F_\ell(\xi) = \int_0^\xi J_\ell(t)\,t\,dt = \xi\,\frac{\Gamma(\ell/2+1)}{\Gamma(\ell/2)}\sum_{k=0}^{\infty}\frac{(\ell+2k+1)\Gamma(\ell/2+k)}{\Gamma(\ell/2+2+k)}\,J_{\ell+2k+1}(\xi)\,. \tag{19}$$

- Equation (19) equals the following closed-form expressions for $1 \le \ell \le 4$:

$$F_1(\xi) = \tfrac{\pi}{2}\xi\left[\mathbf{H}_0(\xi)J_1(\xi) - \mathbf{H}_1(\xi)J_0(\xi)\right]\,, \qquad \ell = 1 \tag{20a}$$

$$F_2(\xi) = 2 - 2J_0(\xi) - \xi J_1(\xi)\,, \qquad \ell = 2 \tag{20b}$$

$$F_3(\xi) = \left[\tfrac{3\pi}{2}\xi\,\mathbf{H}_0(\xi) - 8\right]J_1(\xi) + \left[4\xi - \tfrac{3\pi}{2}\xi\,\mathbf{H}_1(\xi)\right]J_0(\xi)\,, \qquad \ell = 3 \tag{20c}$$

$$F_4(\xi) = 4 - 8J_1(\xi)/\xi - 4J_2(\xi) - \xi J_3(\xi)\,, \qquad \ell = 4 \tag{20d}$$

[4] M. Abramowitz and I. A. Stegun, editors 1972.

Verification of Eq. (18)

- The validity of Eq. (18) is assessed by comparison to

$$q(x, y, z) = \mathcal{F}_{xy}^{-1}\left\{ e^{ik_z z} \mathcal{F}_{xy}[q(x, y, 0)] \right\} , \quad k_z = k - \frac{k_x^2 + k_y^2}{2k} . \qquad (21)$$

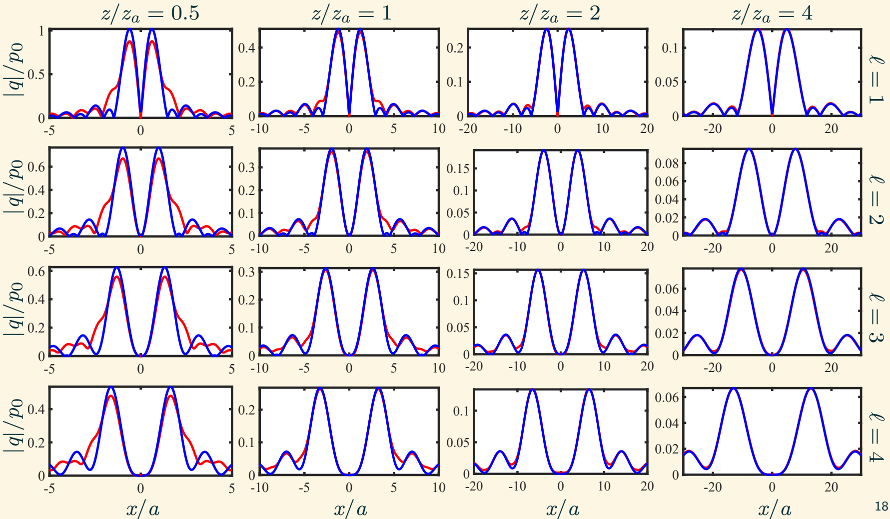

Vortex radiation from focused circular piston

- To describe spherical focusing at a geometric focal length d, source condition (15) is multiplied by $\exp(-ikr^2/2d)$:

$$q(r,\theta,0) = p_0 \,\mathrm{circ}(r/a)\, e^{i\ell\theta} e^{-ikr^2/2d}\,, \tag{22}$$

- An analytical solution of Eq. (2) is available in the focal plane $z = d$:

$$\boxed{q_\ell(r,\theta,d) = -ip_0 \frac{d}{kr^2} e^{ikr^2/2d} e^{i\ell(\theta-\pi/2)} F_\ell(kar/d)\,,} \tag{23}$$

where $F_\ell(\xi)$ is given by Eq. (19).

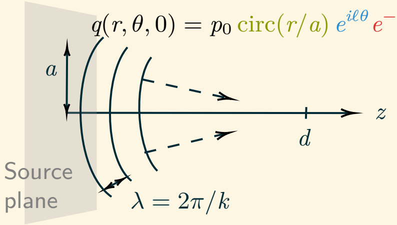

Vortex ring radius

- Extremizing the solutions in r amounts to solving

$$\frac{d|\xi^{-1}F_\ell(\xi)|}{d\xi} = 0\,,$$

  where $\xi = kar/z$ (unfocused) and $\xi = kar/d$ (focused).
- Using Eq. (19) for F_ℓ and taking the derivative yields[5]

$$\sum_{k=0}^{\infty} \frac{(\ell+2k+1)\Gamma(\ell/2+k)}{\Gamma(\ell/2+2+k)} \left[\frac{J_{\ell+2k}(\xi) - J_{\ell+2k+2}(\xi)}{2\xi} - \frac{J_{\ell+2k+1}(\xi)}{\xi^2} \right] = 0\,. \qquad (24)$$

- The roots ξ_ℓ of Eq. (24) are fit to a line:

$$\xi_\ell = 1.23\ell + 1.49\,. \qquad (25)$$

- Solving $\xi_\ell = kar_\ell/z$ and $\xi_\ell = kar_\ell/d$ for r_ℓ yields

$$r_\ell = \frac{\xi_\ell z}{ka}\,, \quad z \gg z_R\,, \qquad (26a)$$

$$= \frac{\xi_\ell d}{ka}\,, \quad z = d\,. \qquad (26b)$$

[5] I. S. Gradshteyn and I. M. Ryzhik, *Table of Integrals, Series, and Products*, 4th ed. Item 8.471-2.

Outline

A simplified diffraction integral

- The angular spectrum method is equivalent to the first Rayleigh integral:

$$p(r,\theta,z) = \rho_0 c_0 k \mathcal{F}_{2\mathrm{D}}^{-1}\{\mathcal{F}_{2\mathrm{D}}\{u_z(r,\theta)\} e^{ik_z z}/k_z\}\,, \tag{27}$$

  where

$$\{\mathcal{F}_{2\mathrm{D}}\{f(r,\theta)\} = \hat{f}(k_r,\psi) = \int_0^\infty \int_0^{2\pi} f(r,\theta) e^{-ik_r r\cos(\theta-\psi)} r\,dr\,d\theta\,, \tag{28a}$$

$$\mathcal{F}_{2\mathrm{D}}^{-1}\{\hat{f}(k_r,\psi)\} = f(r,\theta) = \int_0^\infty \int_0^{2\pi} \hat{f}(k_r,\psi) e^{ik_r r\cos(\theta-\psi)} k_r\,dk_r\,d\psi\,. \tag{28b}$$

- In light of F_ℓ and Watson's relation[6]

$$J_n(\beta) = \frac{1}{2\pi}\int_\alpha^{2\pi+\alpha} e^{i(n\phi-\beta\sin\phi)}\,d\phi\,, \tag{29}$$

  Eq. (27) reduces to

$$p/\rho_0 c_0 u_0 = e^{i\ell\theta}\int_0^\infty (k/k_z) F_\ell(k_r a) J_\ell(k_r r) e^{ik_z z} dk_r/k_r\,. \tag{30}$$

[6] G. N. Watson 1944.

A simplified diffraction integral

- In terms of the dimensionless parameters

$$P \equiv p/\rho_0 c_0 u_0\,, \quad R \equiv r/a\,, \quad Z \equiv z/z_R\,, \quad K \equiv ka\,, \tag{31}$$

where z_R is the Rayleigh distance $ka^2/2$, and where

$$k_z/k = \sqrt{1-(\zeta/K)^2}\,, \quad \zeta \equiv k_r a\,, \tag{32}$$

Eq. (30) becomes

$$P = e^{i\ell\theta} \int_0^\infty \frac{F_\ell(\zeta) J_\ell(\zeta R)}{\zeta\sqrt{1-(\zeta/K)^2}}\, e^{iK^2 Z\sqrt{1-(\zeta/K)^2}/2}\, d\zeta\,. \tag{33}$$

- Equation (33) is equivalent to the Rayleigh integral.

Mr. Jackson S. Hallveld

Dr. Randall P. Williams

Outline

Prefocal shadow zone

- Magnitude of solution of Eq. (2) for focused Gaussian vortex source is

$$|q(r,z)| = \sqrt{8\pi}\,\frac{p_0 z}{kr^2}\left|\chi^{3/2}e^{-\chi}\left[I_{(\ell-1)/2}(\chi) - I_{(\ell+1)/2}(\chi)\right]\right|, \qquad (34)$$

$$\chi(r,z) = \frac{\frac{1}{8}(kar/z)^2}{1 - i(ka^2/2z)(1-z/d)}$$

- For moderate values of focusing gain G, Eq. (34) reveals movement of vortex ring out of focal plane $z = d$ as ℓ increases

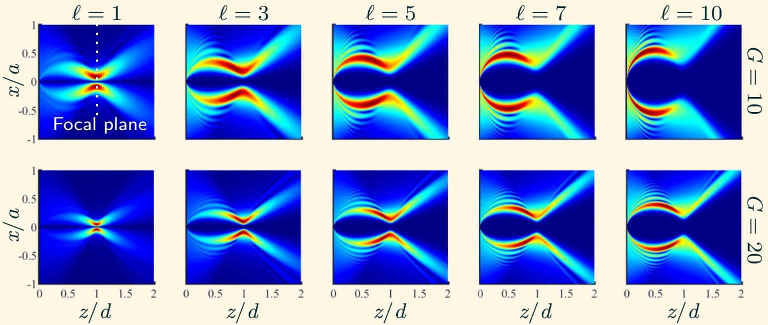

Focused vortex source condition

- To explain this behavior with increasing ℓ, appeal to *ray theory*: $ka \to \infty$
- In homogeneous media, rays travel in straight lines
- In the vicinity of source, pressure field is

$$p(r,\theta,z) \simeq p_0\, f(r)\, e^{i\phi}\,, \quad z \simeq 0$$

  where $f(r) =$ axisymmetric amplitude distribution in source plane
- Phase accounts for focusing, helical wavefronts, and traveling wave motion:

$$\phi(r,\theta,z) = -kr^2/2d + \ell\theta + kz$$

Sunbeams

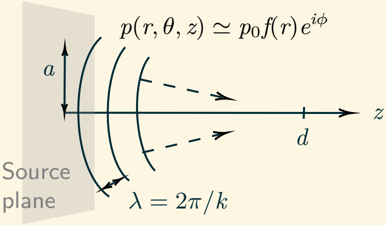

Wave normal $\mathbf{n}$ and annular channel radius Δ

- Wave normal in source plane at distance r_0 from origin is

$$\mathbf{n} = \frac{\boldsymbol{\nabla}\phi}{|\boldsymbol{\nabla}\phi|} = \frac{-(r_0/d)\,\mathbf{e}_r + (\ell/kr_0)\,\mathbf{e}_\theta + \mathbf{e}_z}{\sqrt{(r_0/d)^2 + (\ell/kr_0)^2 + 1}}$$

- Radius of circle formed by family of rays emanating from $r = r_0$ in source plane is

$$\boxed{\Delta(r_0, z) = r_0\left[(1 - z/d)^2 + (\ell d/kr_0^2)^2 (z/d)^2\right]^{1/2}}$$

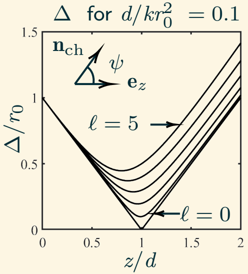

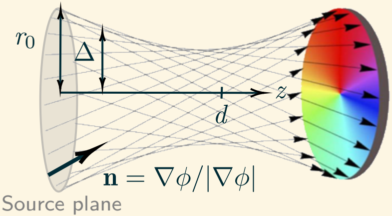

Adapted from G. Richard et al. 2020, *New J. Phys.*

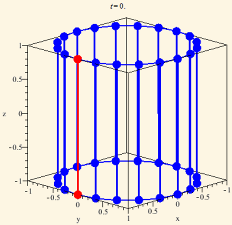

Examples of hyperboloids in architecture

(a) (b) (c)

(a) Water tower in Ciechanów, Poland.[7] (b) The Corporation Street Bridge in Manchester, England.[8] (c) The Essarts-le-Roi water tower, France.[9]

---

[7]Photograph by Henry Salomé, 2006, distributed under a CC-BY 3.0 license.
[8]Photograph by Kaczorgw, 2006, distributed under a CC-BY 3.0 license.
[9]Photograph by Gerald England, 1999, distributed under a CC-BY 2.0 license.

Pressure field according to ray theory

- Pressure field predicted by ray theory:

$$P(\Delta, z) = p_0\, f(r_0) \sqrt{A(r_0, 0)/A(r_0, z)} \tag{35}$$

- Area of annular ray channel is

$$A(r_0, z) = A_z(r_0, z) \cos\psi(r_0, z) = 2\pi w \frac{\Delta(r_0, z)|\partial\Delta/\partial r_0|}{\sqrt{1 + (\partial\Delta/\partial z)^2}} \tag{36}$$

- Inserting Eq. (36) into Eq. (35) and calculating $\partial\Delta/\partial r_0$ and $\partial\Delta/\partial z$ yields

$$P(\Delta, z) = p_0\, f(r_0) \left[\frac{\cos\psi(r_0, 0)/\cos\psi(r_0, z)}{\left|(1 - z/d)^2 - (\ell d/k r_0^2)^2 (z/d)^2\right|} \right]^{1/2}$$

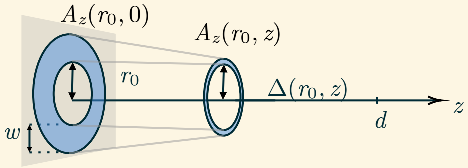

Ray pressure field $P(\Delta, z)$ for $f(r) = e^{-r^2/a^2}$

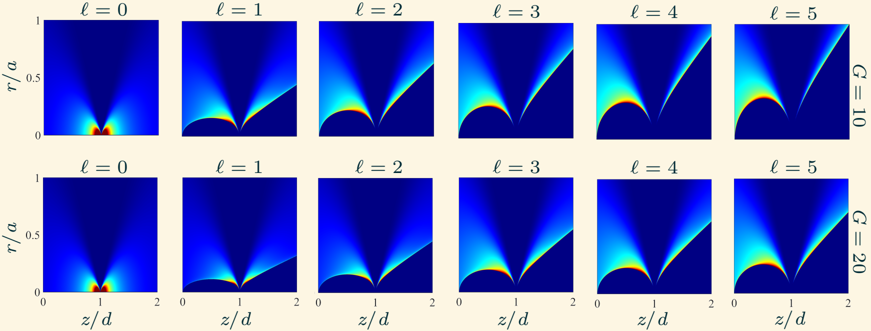

Color plots for the ray field $P(\Delta, z)$ due to a focused Gaussian vortex source.

Caustics

- Caustics occur when cross-sectional area vanishes, i.e.,

$$A_z(r_0, z) = 2\pi r_0 w \left| (1 - z/d)^2 - (\ell d/kr_0^2)^2 (z/d)^2 \right| = 0 \tag{37}$$

- Substitution of roots of Eq. (37) into $\Delta(r_0, z)$ gives caustic coordinates:

$$\boxed{\Delta_c(z) = \sqrt{(2\ell d/k)(z/d)|1 - z/d|}} \tag{38}$$

- Squaring Eq. (38), notating $G = ka^2/2d$, and identifying

$$\Delta_c^2 = x_c^2 + y_c^2\,, \quad a_c^2 = \ell a^2/4G\,, \quad c_c^2 = d^2/4$$

reveals that prefocal caustic is a spheroid of volume $V_c = \frac{1}{6}\ell\lambda d^2$:

$$\boxed{\frac{x_c^2 + y_c^2}{a_c^2} + \frac{(z_c - d/2)^2}{c_c^2} = 1\,, \quad 0 \le z_c \le d}$$

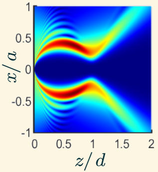

$G = 10$
$\ell = 5$

Prolate for $(d/a)^2 G > \ell$

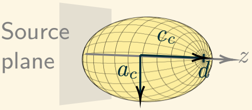

Oblate for $(d/a)^2 G < \ell$

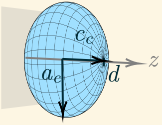

Paraxial field $q(r, z)$, ray paths Δ, and caustics Δ_c

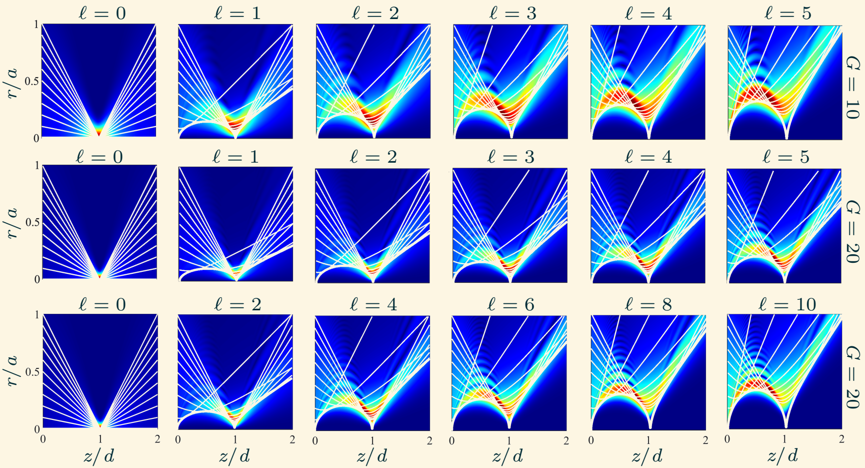

Overlays of caustics Δ_c (thick lines) and ray channels Δ (thin lines) on color plots of the amplitude of the paraxial field $|q(r, z)|$ due to a focused Gaussian vortex source. Rays emanating from $r > a$ have been suppressed for visual clarity.

$q(r, z)$, Δ, and Δ_c for $f(r) = \mathrm{circ}(r/a)$

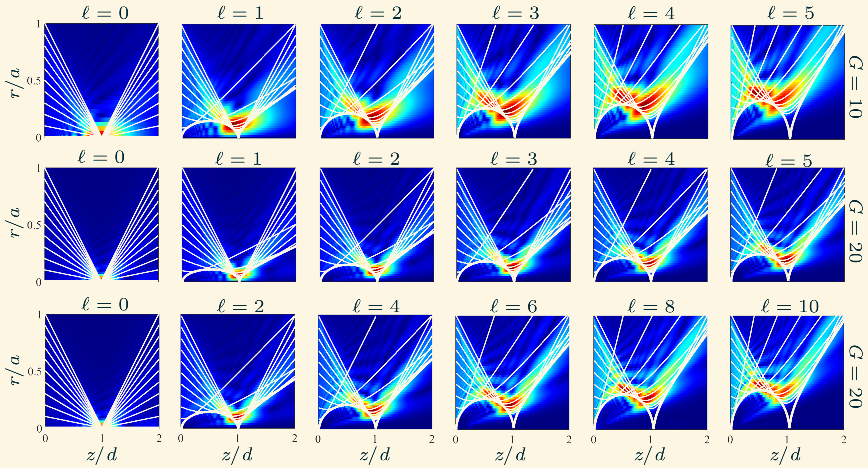

Overlays of caustics Δ_c (thick lines) and ray channels Δ (thin lines) on color plots of the amplitude of the paraxial field $|q(r, z)|$ due to a uniform focused vortex source.

Unfocused limit, $d \to \infty$

- For unfocused vortex beams, $d \to \infty$, for which Δ, Δ_c, and P reduce to

$$\Delta(r_0, z) = r_0[1 + (\ell z/kr_0^2)^2]^{1/2}\,, \quad \text{ray channel radius}$$

$$\Delta_c(z) = \sqrt{2\ell z/k}, \quad \text{caustic radius}$$

$$P(\Delta, z) = p_0 f(r_0)\left[\frac{\cos\psi(r_0,0)/\cos\psi(r_0,z)}{\left|1-(\ell z/kr_0^2)^2\right|}\right]^{1/2}$$

- Caustic surface is a paraboloid, where $z_R = ka^2/2$:

$$\frac{z}{z_R} = \frac{x_c^2 + y_c^2}{\ell a^2}\,, \quad z \geq 0$$

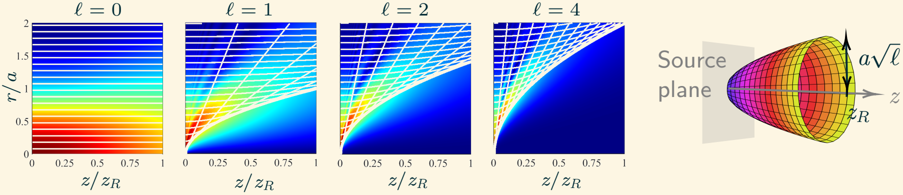

Unfocused limit, $d \to \infty$, $f(r) = \mathrm{circ}(r/a)$

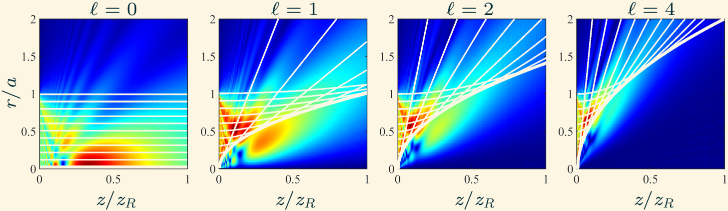

Overlays of caustics Δ_c (thick lines) and ray channels Δ (thin lines) on color plots of the amplitude of the paraxial field $|q(r, z)|$ due to a uniform unfocused vortex source.

Further reading

JASA ARTICLE

Paraxial and ray approximations of acoustic vortex beams

Chirag A. Gokani,[1,2] Michael R. Haberman,[1,2] and Mark F. Hamilton[1,2,a)]
[1]*Applied Research Laboratories, The University of Texas at Austin, Austin, Texas 78766-9767, USA*
[2]*Walker Department of Mechanical Engineering, The University of Texas at Austin, Austin, Texas 78712-1063, USA*

(Received 19 January 2024; revised 27 March 2024; accepted 27 March 2024; published online 22 April 2024)
[Editor: Philip L. Marston] Pages: 2707–2723

J. Acoust. Soc. Am. **155** (4), April 2024

Outline

Motivation to study nonlinear problem

New Journal of Physics (2020)

The open access journal at the forefront of physics

Published in partnership with: Deutsche Physikalische Gesellschaft and the Institute of Physics

PAPER

Twisting waves increase the visibility of nonlinear behaviour

Grace Richard[1], Holly S Lay[1], Daniel Giovannini[1], Sandy Cochran[1], Gabriel C Spalding[2] and Martin P J Lavery[1,3]

[1] School of Engineering, University of Glasgow, Glasgow, United Kingdom
[2] Department of Physics, Illinois Wesleyan, Bloomington, IL 61702, United States of America
[3] Author to whom any correspondence should be addressed.

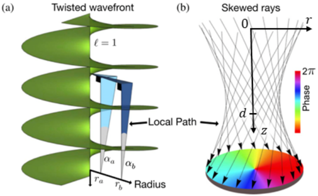

Hypothesis:

- Wavefronts travels farther than they would in the absence of vorticity.
- The phase evolves more rapidly in z direction due to the extra path length.
- Cumulative nonlinear effects in z direction occur over a shortened length scale.

Geometry of Bessel vortex beam

- The Bessel vortex beam is simply a cylindrical eigenfunction of the Helmholtz equation:

$$p(r, \theta, z) = p_0 J_\ell(k_r r) e^{i(k_z z + \ell\theta)} \,. \tag{39}$$

- The surface of constant phase is $\Phi(z, \theta) = k_z z + \ell\theta$.
- The wave normal is

$$\mathbf{n} = \frac{\boldsymbol{\nabla}\Phi}{|\boldsymbol{\nabla}\Phi|} = \frac{k_z r \mathbf{e}_z + \ell \mathbf{e}_\theta}{\sqrt{(k_z r)^2 + \ell^2}} \,. \tag{40}$$

- The angle with respect to the z axis is $\tan\phi = \ell / k_z r$.

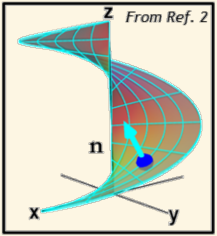

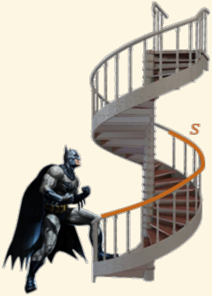

Attempted reduction to 1D

- Over the coordinate $s = z/\cos\phi$, the Burgers equation is

$$\frac{\partial p}{\partial s} - \frac{\delta}{2c_0^2}\frac{\partial^2 p}{\partial \tau^2} = \frac{\beta p}{\rho_0 c_0^3}\frac{\partial p}{\partial \tau}\,. \tag{41}$$

- The reduced shock-formation distance is

$$\bar{z} = \frac{\cos\phi}{\beta k \epsilon(r)} = \frac{k_z r}{\sqrt{(k_z r)^2 + \ell^2}}\frac{1}{\beta k \epsilon(r)}\,. \tag{42}$$

- The Fubini solution over normalized coordinate $\sigma = s/\bar{z}$ is

$$\begin{aligned} p(\sigma,\theta) &= p_0 \sum_{n=1}^{\infty} \frac{2}{n\sigma} J_n(n\sigma)\sin n\omega\tau \\ &= p_0 \sum_{n=1}^{\infty} B_n(\sigma)\sin n\omega\tau\,, \\ B_1 &= 1 + \mathcal{O}(\sigma^2) \\ B_2 &= \tfrac{1}{2}\sigma + \mathcal{O}(\sigma^3) \\ B_3 &= \tfrac{3}{8}\sigma^2 + \mathcal{O}(\sigma^4) \\ B_4 &= \tfrac{1}{3}\sigma^3 + \mathcal{O}(\sigma^5)\,. \end{aligned}$$

Numerical solution of Westervelt equation

Westervelt equation in retarded time[1]

$$\frac{\partial^2 p}{\partial \tau \partial z} = \underbrace{\frac{c_0}{2}\nabla^2 p}_{\text{diffraction}} + \underbrace{\frac{\beta}{2\rho_0 c_0^3}\frac{\partial^2 p^2}{\partial \tau^2}}_{\text{nonlinearity}} + \underbrace{\frac{\delta}{2c_0^3}\frac{\partial^3 p}{\partial \tau^3}}_{\text{absorption}}$$

$\tau = t - z/c_0$

Inputs parameters

ℓ	orbital number	+ source condition
ka	ratio of source size to wavelength	
B	ratio of diffraction to nonlinearity	
A	ratio of attenuation to diffraction	

Numerical solution based on operator splitting[1,2]

Diffraction: $\frac{\partial^2 p}{\partial \tau \partial z} = \frac{c_0}{2}\nabla^2 p$ → Fourier acoustics:

$$p_n(x,y,z+\Delta z) = \mathcal{F}_{2D}^{-1}\left\{\exp\left(i\sqrt{k_n^2 - k_x^2 - k_y^2}\Delta z - ik_n\Delta z\right)\mathcal{F}_{2D}[p_n(x,y,z)]\right\}$$

Nonlinearity: $\frac{\partial p}{\partial z} = \frac{\beta}{2\rho_0 c_0^3}\frac{\partial p^2}{\partial \tau}$ → Runge-Kutta 4th order method:

$$\frac{\partial p_n}{\partial z} = \frac{in\beta\omega}{\rho_0 c_0^3}\left(\sum_{k=1}^{N_{\max}-n} p_k p_{n+k}^* + \frac{1}{2}\sum_{k=1}^{n-1} p_k p_{n-k}\right)$$

Absorption: $\frac{\partial p}{\partial z} = \frac{\delta}{2c_0^3}\frac{\partial^2 p}{\partial \tau^2}$ → Exponential decay:

$$p_n(x,y,z+\Delta z) = p_n(x,y,z)\exp[-(\omega_n^2\delta/2c_0^3)\Delta z]$$

[1] Yuldashev and Khokhlova, Acoustical Physics (2011)
[2] Lee and Hamilton, JASA (1995)

Numerical solution for Bessel vortex beam

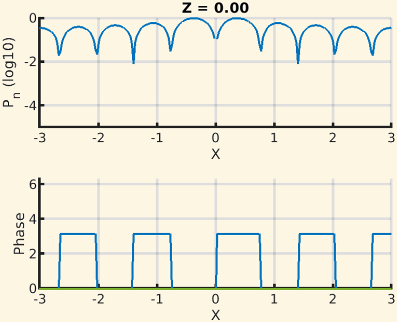

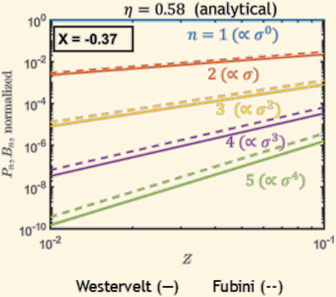

$\phi = 1.5°$ for these parameters

Outline

Thank you for listening!

Summary

- Solved Eq. (2) for Gaussian and uniform vortex sources
- Calculated scaling laws for both solutions
- Derived simplified integral solution of Helmholtz equation for pistons
- Developed ray theory to explain behavior of field with increasing ℓ
- Showed that shadow zone in prefocal region is a spheroid
- Calculated pressure field from ray theory

Acknowledgments

- Chester M. McKinney Graduate Fellowship in Acoustics at the Applied Research Laboratories

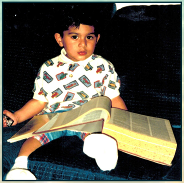

Mr. Chirag Gokani

Prof. Michael Haberman

Prof. Mark Hamilton

References I

- C. Shi et al. (2017). "High-speed acoustic communication by multiplexing orbital angular momentum". *P. Natl. Acad. Sci. U.S.A.* 114, pp. 7250–7253.
- B. T. Hefner and P. L. Marston (1999). "An acoustical helicoidal wave transducer with applications for the alignment of ultrasonic and underwater systems". *J. Acoust. Soc. Am.* 106, pp. 3313–3316.
- M. E. Terzi et al. (2017). "Generation of a vortex ultrasonic beam with a phase plate with an angular dependence of the thickness". *Moscow University Physics Bulletin* 72, pp. 61–67.
- A. Marzo, M. Caleap, and B. W. Drinkwater (2018). "Acoustic virtual vortices with tunable orbital angular momentum for trapping of mie particles". *Phys. Rev. Lett.* 120, pp. 1–6.
- X. Jiang et al. (2016). "Convert acoustic resonances to orbital angular momentum". *Phys. Rev. Lett.* 117, pp. 1–5.
- N. Jiménez, J. -P. Groby, and V. Romero-García (2021). "Spiral sound-diffusing metasurfaces based on holographic vortices". *Sci. Rep.* 11, pp. 1–13.

References II

Zhang, L. and P. L. Marston (2011). "Angular momentum flux of nonparaxial acoustic vortex beams and torques on axisymmetric objects". *Phys. Rev. E* 84, pp. 1–5.

M. E. Kelly and C. Shi (2023). "Design and simulation of acoustic vortex wave arrays for long-range underwater communication". *JASA Express Lett.* 3, pp. 1–5.

S. Guo et al. (2022). "Enhanced Sonothrombolysis Induced by High-Intensity Focused Acoustic Vortex". *Ultrasound Med. Biol.* 48, pp. 1907–1917.

D. Baresch, J. -L. Thomas, and R. Marchiano (2016). "Observation of a single-beam gradient force acoustical trap for elastic particles: Acoustical tweezers". *Phys. Rev. Lett.* 116, pp. 1–6.

C. Zhou et al. (2020). "Focused acoustic vortex generated by a circular array of planar sector transducers using an acoustic lens, and its application in object manipulation". *J. Appl. Phys.* 128, pp. 1–12.

V. V. Kotlyar, A. A. Kovalev, and A. P. Porfirev (2018). *Vortex Laser Beams*. , Chaps. 2, 6, and 9. CRC Press.

M. Abramowitz and I. A. Stegun, editors (1972). *Handbook of Mathematical Functions, 4th edition*., Item 11.1.1. New York: Dover Publications.

References III

- G. N. Watson (1944). *A Treatise on the Theory of Bessel Functions, 2nd edition*. Sec. 2.2, Eq. (5). Cambridge, UK: Cambridge University Press.
- G. Richard et al. (2020). "Twisting waves increase the visibility of nonlinear behaviour". *New J. Phys.* 22, pp. 1–8.
- D. Marcuse (1982). *Light Transmission Optics*. 135 West 50th Street, New York, N.Y.: Van Nostrand Reinhold.
- A. D. Pierce (2019). *Acoustics, 3rd edition*. Secs. 8.2 and 8.5. Cham, Switzerland: Springer.

Notation I

Symbol	Description	Dimensions
a	source radius	m
c_0	linear speed of sound	m s^{-1}
d	focal length	m
G	focusing gain	1
i	complex unit	1
$\mathbf{k}$	wavenumber	m^{-1}
ℓ	orbital number	1
ρ_0	ambient mass density	kg m^{-3}
p	acoustic pressure	kg m^{-1} s^{-2}
q	paraxial pressure	kg m^{-1} s^{-2}
$\mathbf{R}$	separation vector $\mathbf{R} = \mathbf{r} - \mathbf{r}'$	m
$\mathbf{r}$	position vector	m
$\mathbf{v}$	particle velocity	m s^{-1}
ω	angular frequency, $\omega = 2\pi f$	s^{-1}
$*$	complex conjugation	
$\cdot$	inner product	
$:$	double inner product	
$\times$	cross product	

Notation II

$\otimes$	outer product	
$\boldsymbol{\nabla}$	gradient	m^{-1}
$\boldsymbol{\nabla}\cdot$	divergence	m^{-1}
$\boldsymbol{\nabla}\times$	curl	m^{-1}
∇^2	Laplacian	m^{-2}
$\boldsymbol{\nabla}^2$	vector Laplacian	m^{-2}
$\langle f(x)\rangle$	average of f over quantity x, $\frac{1}{x}\int f(x)\,dx$	units of f
$\oint_{\partial\Omega} dA$	integral over closed surface	m^2
$\int_{\Omega} dV$	integral over volume	m^3

The big picture[10]

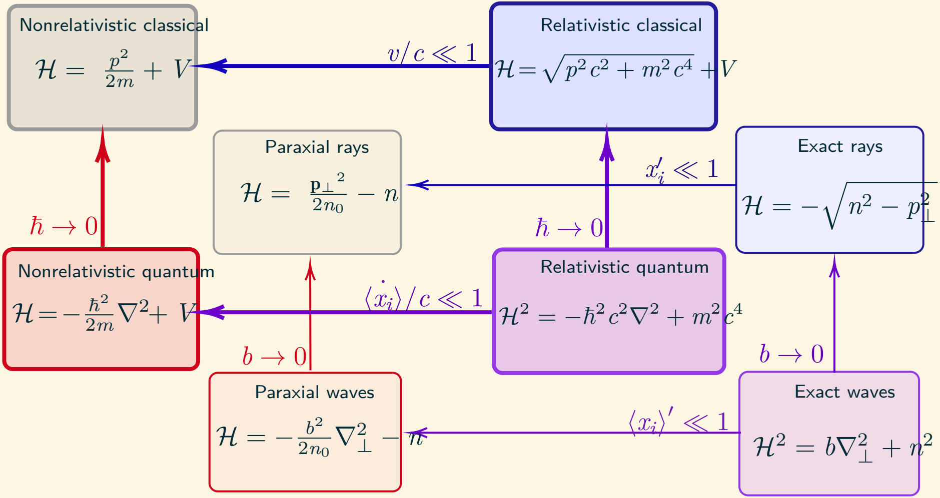

---

[10] D. Marcuse 1982.

Pressure field from ray theory

- Inserting $p(\mathbf{x}) = P(\mathbf{x},\omega)e^{i\omega\tau(\mathbf{x})}$ into $\nabla^2 p + k^2 p = 0$ yields[11]

$$\nabla^2 P + i\omega[2\boldsymbol{\nabla} P \cdot \boldsymbol{\nabla}\tau + P\nabla^2\tau] - \omega^2 P[(\boldsymbol{\nabla}\tau)^2 - c^{-2}] = 0\,. \qquad (8.5.1)$$

- In limit that $\omega \to \infty$, it is necessary for $(\boldsymbol{\nabla}\tau)^2 = c^{-2}$ and

$$\boldsymbol{\nabla}\cdot(P^2\boldsymbol{\nabla}\tau) = 0 \qquad (8.5.3b)$$

- Areas $A(\mathbf{x}_0)$ and $A(\mathbf{x})$ define the end caps of a *ray tube*

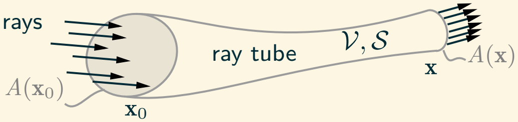

- Integrating Eq. (8.5.3b) over $\mathcal{V}$ and applying Gauss's theorem yields

$$\oint_{\mathcal{S}} (P^2\boldsymbol{\nabla}\tau)\cdot\mathbf{n}\,dS = 0 \implies \boxed{P(\mathbf{x}) = P(\mathbf{x}_0)\sqrt{A(\mathbf{x}_0)/A(\mathbf{x})}\,.}$$

[11] Equation numbers refer to those in *Acoustics*, A. D. Pierce 2019.